

# FreeOcc: Training-free Panoptic Occupancy Prediction via Foundation Models

Andrew Caunes<sup>1,2</sup>, Thierry Chateau<sup>1</sup>, and Vincent Frémont<sup>2</sup>

<sup>1</sup> Logiroad, Nantes, France

<sup>2</sup> LS2N - Ecole Centrale de Nantes, France

**Abstract.** Semantic and panoptic occupancy prediction for road scene analysis provides a dense 3D representation of the ego vehicle’s surroundings. Current camera-only approaches typically rely on costly dense 3D supervision or require training models on data from the target domain, limiting deployment in unseen environments. We propose FreeOcc, a training-free pipeline that leverages pretrained foundation models to recover both semantics and geometry from multi-view images. FreeOcc extracts per-view panoptic priors with a promptable foundation segmentation model and prompt-to-taxonomy rules, and reconstructs metric 3D points with a reconstruction foundation model. Depth- and confidence-aware filtering lifts reliable labels into 3D, which are fused over time and voxelized with a deterministic refinement stack. For panoptic occupancy, instances are recovered by fitting and merging robust current-view 3D box candidates, enabling instance-aware occupancy without any learned 3D model. On Occ3D-nuScenes, FreeOcc achieves 16.9 mIoU and 16.5 RayIoU train-free, on par with state-of-the-art weakly supervised methods. When employed as a pseudo-label generation pipeline for training downstream models, it achieves 21.1 RayIoU, surpassing the previous state-of-the-art weakly supervised baseline. Furthermore, FreeOcc sets new baselines for both train-free and weakly supervised panoptic occupancy prediction, achieving 3.1 RayPQ and 3.9 RayPQ, respectively. These results highlight foundation-model-driven perception as a practical route to training-free 3D scene understanding.

**Keywords:** 3D occupancy prediction · Panoptic occupancy · Foundation models · Training-free inference · Autonomous driving

## 1 Introduction

Understanding and predicting the 3D structure of road scenes is a cornerstone of autonomous driving and road infrastructure analysis. While active sensors such as LiDAR provide accurate geometry, they increase system cost and are not always available, motivating camera-only perception as a scalable alternative.

However, recovering metric 3D structure from RGB is inherently ambiguous: depth is only indirectly observable, and occlusions, long-range geometry, and dynamic actors further challenge dense 3D reasoning.

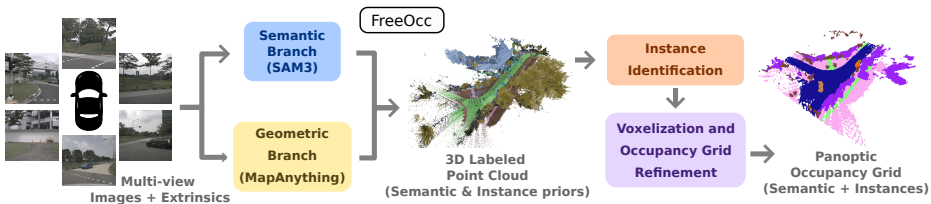


**Fig. 1: FreeOcc: Training-free panoptic occupancy prediction from foundation models.** The pipeline operates directly from camera images and poses without any training. It combines a Semantic Branch powered by the SegmentAnything foundation model (SAM3) and a Geometric Branch powered by the MapAnything 3D reconstruction model to obtain 3D semantically labeled point clouds with instance priors from SAM3’s masks. An Instance Identification module then refines instance candidates and re-assigns wrongly labeled points to the correct instance and semantic class. Finally, the fused point cloud is voxelized and refined to produce the final panoptic occupancy grid.

3D occupancy prediction addresses this by discretizing the ego-centric scene into a voxel grid and estimating which voxels are occupied, often with semantic labels; its panoptic variant additionally assigns instance identifiers to “thing” classes. Benchmarks such as Occ3D [13] have standardized evaluation for camera-based semantic occupancy.

Most high-performing approaches rely on dense 3D supervision, typically generated from LiDAR annotation accumulation and post-processing. Such supervision is costly to acquire and limits scaling to new domains, sensor configurations, and evolving taxonomies for semantic classes.

This has spurred weakly supervised alternatives that reduce manual 3D labeling by leveraging geometric priors and pseudo-labels. In particular, GaussianFlowOcc [1] and ShelfOcc [2] demonstrate that foundation-model-driven cues can provide useful supervision for occupancy learning, yet they still depend on training a target-domain occupancy network and focus primarily on semantic occupancy.

We propose FreeOcc, a foundation-model pipeline that pushes this paradigm to the limit: FreeOcc performs *training-free* semantic *and* panoptic occupancy prediction directly at inference time. It requires no target-domain images prior to deployment, can be run in a new domain without any optimization, and inherits the open-vocabulary capabilities of foundation models, allowing it to adapt its label space by changing text prompts rather than retraining a 3D model.

The main cost of eliminating training is compute: running large 2D and 3D foundation models makes inference slower than a specialized network. We therefore position FreeOcc first as a stand-alone train-free predictor for rapid deployment that can alternatively be used as a high-quality pseudo-label generator for training downstream real-time occupancy models when target data becomes available.

Concretely, FreeOcc combines a promptable segmentation foundation model (SAM [9]; we use SAM3) to extract per-view semantic/instance masks with confidences, and a metric reconstruction model (MapAnything [8]) that outputs dense per-pixel 3D points along with depth and confidence maps. Depending on the application, this pipeline can be applied both in a causal and non-causal manner, by either only using past and current frames, or all available frames. After confidence-aware filtering, reliable per-pixel 3D points are assigned semantic and instance labels, fused over time, and converted into a voxel grid with a deterministic multi-stage refinement stack. For panoptic occupancy, we fit and merge robust 3D box candidates from current-view thing evidence to assign consistent instance ids in the fused cloud prior to voxelization.

On Occ3D-nuScenes [13], FreeOcc achieves 16.9 mIoU and 16.5 RayIoU for semantic occupancy without any training (Table 1), substantially improving over prior train-free results (e.g., ShelfOcc at 9.6 mIoU [2]). Despite being train-free, our semantic results are competitive with trained weakly supervised occupancy methods such as GaussianFlowOcc [1]. For comparison purposes, we also train downstream occupancy models on pseudo-labels generated by FreeOcc, following [2], and reach state-of-the-art weakly supervised performance with 21.1 RayIoU. For panoptic occupancy, we report the first training-free and weakly supervised results on Occ3D-nuScenes, with a training-free baseline at 3.1 RayPQ and a weakly supervised transfer result at 3.9 RayPQ, highlighting both the feasibility of instance-aware label-free occupancy and the remaining gap to fully supervised predictors [11, 16]. We further provide an ablation study and detailed analysis of the impact of each pipeline component. **Our main contributions are the following:**

- **Training-free.** We introduce FreeOcc, a training-free occupancy prediction pipeline that matches or surpasses trained weakly supervised baselines. A multi-stage refinement of foundation-model outputs allows it to reach 16.9 mIoU and 16.5 RayIoU for semantic occupancy on Occ3D-nuScenes without any training or target data.
- **Pseudo-label generation.** It can also be used as a pseudo-label generator for training downstream occupancy models for real-time inference. In this setting, it achieves state-of-the-art performance: 22.8 mIoU and a 21.1 RayIoU for semantic occupancy, without the use of visibility masks during training.
- **Panoptic occupancy.** Using an efficient instance identification module, FreeOcc can also output robust instance predictions. It achieves 3.1 RayPQ (train-free) and 3.9 RayPQ (weakly supervised) on Occ3D-nuScenes, setting new baselines for both regimes.

## 2 Related works

### 2.1 3D Occupancy Prediction

Camera-based 3D occupancy prediction estimates a voxelized representation of the scene from multi-view images and calibrated poses, with semantic labels

assigned to occupied voxels. Voxels in a fixed grid are more straightforward to predict from 2D images than unstructured point clouds, making this the natural setting for camera-only prediction methods. Panoptic occupancy extends this setting by adding instance identifiers for “thing” classes, combining volumetric semantics and instance-level scene decomposition in a single output. Occ3D [13] standardized the semantic occupancy prediction task at scale, and later works further emphasized panoptic occupancy prediction with ray-based evaluation metrics for better geometric fidelity analysis [11].

Most high-performing camera-only methods on Occ3D are trained with dense 3D voxel labels. Representative architectures include dense volumetric lifting and 3D refinement pipelines [15], and sparse formulations that avoid dense 3D reasoning via sparse reconstruction and query-based prediction [11]. In parallel, several works explore alternative 3D feature parameterizations, e.g., multi-plane (tri-plane/TPV-style) representations [6], which have been adopted by later occupancy systems. More recent systems revisit the output space itself, e.g., set prediction formulations [14]. Temporal reasoning is a major performance driver, with STCOcc [10] showing strong gains via explicit sparse spatial-temporal cascade renovation.

Panoptic occupancy prediction is harder and has been less explored than semantic occupancy as it requires both 3D geometric consistency and instance-aware grouping in a voxelized space. SparseOcc [11] is a strong fully-supervised baseline and formalized a panoptic evaluation benchmark with the ray-based RayPQ metric. Panoptic-FlashOcc [16] targets efficiency with a streamlined design that combines semantic occupancy with instance-center prediction and lightweight panoptic assignment.

## 2.2 Weakly Supervised / Training-Free Paradigms

To reduce reliance on dense 3D voxel supervision, prior works explored several regimes that trade 3D GT for weaker signals.

Some methods replace 3D voxel GT with supervision available in the image plane (e.g., semantic labels/depth maps), typically implemented via differentiable rendering/projection losses [12]. While avoiding dense 3D annotations, these approaches still rely on labeled 2D datasets.

A related line keeps the same 2D training paradigm but replaces human 2D labels by pseudo-labels produced by off-the-shelf models (e.g., 2D semantics/depth) and/or self-supervised multi-view/video consistency losses. This includes GaussianFlowOcc [1] as well as NeRF-/Gaussian-based variants and foundation-model alignment schemes [4, 7, 17].

Most closely related to our setting, two recent preprints, EasyOcc [5] and ShelfOcc [2] proposed to leverage foundation-model priors to generate 3D voxel pseudo-labels, which are then used to train a downstream occupancy network. For fairness, we include and compare against them in our experiments using their reported results. ShelfOcc [2] in particular leverages off-the-shelf geometric and semantic foundation models to build metrically consistent 3D voxel pseudo-labels, which are then used to train a downstream model. Our approach also leverages

similar foundation models to obtain 3D occupancy predictions. Differently from ShelfOcc, FreeOcc is not pseudo-label focused. Instead, we introduce multiple innovations to refine predictions such as a semantic prompt & rules system, a multi-stage occupancy grid refinement module, and an instance identification module to re-assign instance and semantic labels. These innovations allow our method to reach competitive performance with ShelfOcc without their training scheme.

In contrast to all trained pipelines above, FreeOcc operates directly at inference time without any downstream training. This enables deployment to new environments without a separate data-collection and training phase. This setting also better preserves the open-vocabulary potential of foundation models as target classes can be picked on-the-fly at inference time. When real-time inference is required, our pipeline can still be used as a pseudo-label generator for downstream training. We demonstrate this in our experiments for direct comparison with ShelfOcc [2] and EasyOcc [5].

Finally, existing weakly supervised works have focused on semantic occupancy prediction; to our knowledge, our method is the first to establish baselines for both weakly supervised and training-free panoptic occupancy prediction.

### 3 Method

An overview of FreeOcc can be seen in Fig. 1. Its main stages are illustrated in Figs. 2–5 and explained in the following subsections.

#### 3.1 Problem Setup

We consider multi-camera samples  $\{\mathcal{X}_t\}_{t=1}^T$  with  $\mathcal{X}_t = \{(I_t^c, K_t^c, T_t^c)\}_{c=1}^C$ , where  $I_t^c$  is the image from camera  $c$ , and  $K_t^c, T_t^c$  are the corresponding intrinsics and extrinsics.

Our output at time  $t$  is a semantic occupancy grid  $\mathbf{Y}_t^{\text{sem}}$  and an instance-id grid  $\mathbf{Y}_t^{\text{ins}}$  defined on a fixed ego-centric voxel lattice. The pipeline is training-free and can be run either non-causally (offline) or causally; causality is enforced by restricting which frames are used to build the 3D evidence for time  $t$ . We denote by  $\mathcal{W}_t \subseteq \{1, \dots, T\}$  the set of frame indices used to build 3D evidence for time  $t$ . In the causal setting,  $\mathcal{W}_t \subseteq \{1, \dots, t\}$ .

#### 3.2 Prompted 2D Priors from SAM3

The semantic branch details are illustrated in Fig. 2. **Semantic prompts.** We prompt a segmentation foundation model (SegmentAnything [9]; we use SAM3) with a handcrafted prompt set  $\mathcal{P}$ , which is easily derived from the target taxonomy labels. This set includes synonyms intended to be more common for the model than the class name. For example, for the class “terrain”, we use the prompts “grass” and “dirt”, yielding high-quality masks, while the “terrain” prompt is misunderstood. Similarly, the “manmade” class is too vague, while “building”

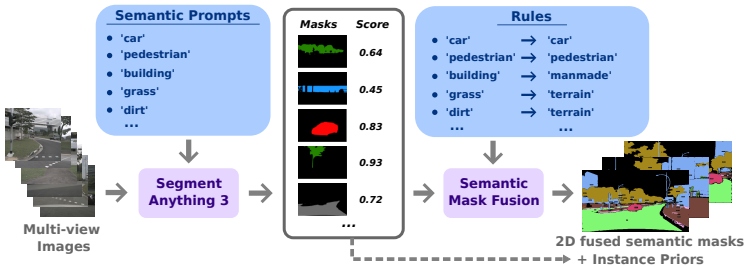


**Fig. 2: Semantic branch.** A set of easily handcrafted prompts is fed to SegmentAnything3 [9], which yields 2D mask candidates with scores; we fuse them into per-view semantic and instance priors and use rules to remap prompt classes to the target taxonomy. Multiple prompts can be used for each target class, e.g. synonyms.

and “wall” are more specific and yield better results. We use 25 prompts in total for the 15 Occ3D classes (excluding ‘others’ and ‘other\_flat’). The prompt set we use for the Occ3D-nuScenes taxonomy is provided in the Supplementary Material. We show how naive class-name prompts affect performance significantly in the ablation study in Sec. 4.

**Fusing masks.** For each view, SAM3 produces multiple mask candidates per prompt, each with a score. In this subsection, we omit the view index  $(t, c)$  for clarity: all quantities are per-view. For each prompt  $k$  and candidate index  $m$ , SAM3 outputs a binary mask  $M_k^{(m)}$  over the image domain with confidence score  $s_k^{(m)}$ . We fuse candidates into a single semantic mask  $\hat{S}(u)$  and an instance prior mask  $\hat{U}(u)$  by keeping the highest-scoring candidate covering each pixel:

$$(\hat{k}, \hat{m})(u) = \arg \max_{k, m: u \in M_k^{(m)}} s_k^{(m)}. \quad (1)$$

**Applying rules.** Finally, we remap the winning prompt label to the target taxonomy with simple mapping rules  $r$ :

$$\hat{S}(u) = r(\hat{k}(u)), \quad \hat{U}(u) = \hat{m}(u). \quad (2)$$

This remapping collapses fine-grained prompts into target classes; for example, “grass” → “terrain” and “building” → “manmade”.

For the Occ3D-nuScenes taxonomy, the rule system is purely a prompt-to-taxonomy mapping, but there may also be cases of conflicts between classes, e.g. if the target taxonomy contains “road” and “lane marking”, SAM3 may include lane markings in the “road” masks. In addition, the confidence score for “road” may tend to be higher than for “lane marking” because of the larger area. In these cases, rules can also incorporate “over”/“under” relations between classes that will override the confidence score priority.

### 3.3 Metric 3D Reconstruction and Reliability Filtering

The geometric branch details are illustrated in Fig. 3.

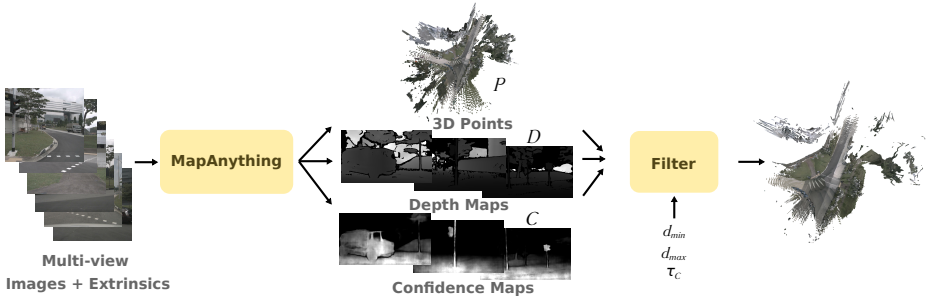


**Fig. 3: geometric branch.** In parallel, MapAnything outputs per-pixel 3D points along with depth and confidence maps. We filter points by depth/confidence and keep the remaining labeled 3D points, yielding a sparse point cloud.

A pretrained geometry model (MapAnything [8]) predicts per-view 3D points, depth and confidence:

$$(P, D, C) = \mathcal{G}(I, K, T). \quad (3)$$

For filtering, confidence is stabilized by replacing non-finite values and applying log scaling:

$$\tilde{C}(u) = \begin{cases} \log_{10}(C(u)) + 1, & C(u) \in \mathbb{R}_+ \text{ finite,} \\ 1, & \text{otherwise,} \end{cases} \quad (4)$$

We normalize confidence and use distance thresholds  $d_{\min}$ ,  $d_{\max}$  and confidence threshold  $\tau_C$  to filter unreliable points:

$$\Omega = \{u : \tilde{C}(u) \geq \tau_C, d_{\min} \leq D(u) \leq d_{\max}\}. \quad (5)$$

Each valid pixel yields a labeled 3D point, which inherits  $(\hat{S}(u), \hat{U}(u))$  as its semantic label and instance prior from the semantic branch. This yields labeled point sets for all frames considered in  $\mathcal{W}_t$ .

### 3.4 Instance Identification via Current-Sample 3D Candidates

This stage is visualized in Fig. 4. Temporal fusion improves static structure but can create ghosting when dynamic thing instances move. We therefore identify instances using current-sample evidence only. Instance priors derived from SAM3’s masks are good candidates for final instances. Noise can however appear from overlap between the multiple cameras and projection bleeding due to imprecise masks / extrinsics. We use an instance identification module to filter out such noise and derive final instances. This module can also improve semantic performance by de-assigning outliers.

**3D Box Fitting.** We start with fitting yaw-oriented 3D boxes to all current-sample instance priors (3D points designated by a single mask). We estimate the ground-plane orientation from PCA in the horizontal plane and take tight extents in the rotated frame ( $SE(2)$ -like yaw + translation).

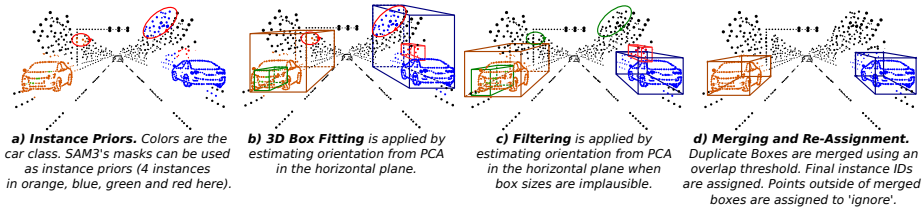


**Fig. 4: instance identification.** Prompted SAM3 yields 2D mask candidates with scores; we fuse them into per-view semantic and instance priors and remap prompts to a canonical taxonomy with a simple lookup. MapAnything yields metric depth with a confidence signal; after reliability filtering we lift pixels to labeled 3D points. We optionally fuse points over time (non-causal or causal by frame selection), regularize thing instances via current-sample 3D box candidates, then voxelize and refine to produce semantic and panoptic occupancy grids.

**Filtering.** For each candidate box, we compare its size with class-wise plausible size intervals, e.g. a 5m area is implausible for a “pedestrian” class. Exact intervals are given in the Supplementary Material. We then discard depth outliers with an interquartile-range (IQR) rule (optionally per camera/view), and prune geometric outliers using a PCA-based robust deviation test in the projected space. When a candidate still produces an implausibly large box, we iteratively tighten these robust thresholds and refit for a few iterations (max. 4) until the box becomes coherent or we reach a maximum number of passes.

**Merging.** Same-class candidate boxes are then merged conservatively to avoid duplicates, based on 3D intersection-over-smaller-volume (IoSV) overlap: we merge boxes only when a large fraction of the smaller box is covered by the other, controlled by threshold  $\tau_{ov}$ .

**Re-assignment.** Finally, we assign one final instance id per merged box and reassign fused thing points: points inside a box take its id; uncovered points are assigned to the nearest box if their point-to-box distance is below  $d_{nn} = 2m$ ; otherwise they are relabeled as ‘ignore’. This produces a fused cloud with more consistent thing instances prior to voxelization. Stuff voxels receive canonical class-level ids.

### 3.5 Occupancy Grids and Refinement

The voxelization and refinement stages are illustrated in Fig. 5. We crop the fused cloud to the occupancy-grid bounds and voxelize it with voxel size  $s_v$  on a grid of size  $(X, Y, Z)$  with vertical offset  $z_0$ .

**Voxelization by voting.** Each point is mapped to a voxel index, and each voxel is assigned a semantic label by majority voting over the point labels while excluding ‘ignore’ votes. Voxels with no non-ignore votes are assigned the ‘free’ class. We keep voxels even with very few points ( $n_{\min} = 1$ ), as noisy returns

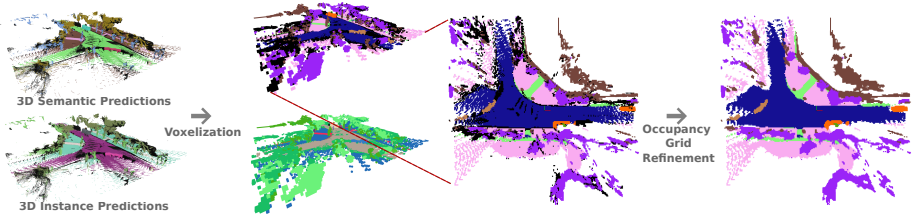


**Fig. 5: voxelization branch.** We voxelize the labeled point cloud and apply a lightweight multi-stage refinement step to produce semantic and panoptic occupancy grids. Notice that small holes, ego vehicle noise and backgrounded ghost artifacts are removed in this stage.

are already reduced by the per-view minimum-distance filtering applied after reconstruction.

**Voxel evidence: support and confidence.** For each occupied voxel  $v$ , we record its *point support*  $n(v)$ , i.e., the number of points that voted for it, and we compute a smoothed vote confidence for the winning class  $c^*(v)$ :

$$\text{conf}(v) = \frac{n_{c^*}(v) + \alpha}{n(v) + \alpha K},$$

where  $n_{c^*}(v)$  is the winning vote count,  $K$  is the number of semantic classes, and  $\alpha$  is a small Dirichlet smoothing constant (we use  $\alpha = 0.5$ ). We also convert point support into a saturating reliability score  $p_{\text{occ}}(v) = 1 - \exp(-\lambda n(v))$  (with  $\lambda = 0.35$ ), which quickly approaches 1 for high-support voxels.

**Refinement stack.** We apply a deterministic four-stage refinement that improves local consistency without over-smoothing. Let  $\mathcal{N}_{26}(v)$  denote the  $3 \times 3 \times 3$  neighborhood around  $v$  (excluding  $v$ ). The *modal class* is the most frequent semantic label in  $\mathcal{N}_{26}(v)$ , and the *modal support* is its vote count (number of neighbors carrying that label). We also denote by  $n_{\text{occ}}(v)$  the number of non-unknown neighbors.

**(1) Pinhole and cavity filling.** We close tiny empty holes inside locally occupied regions using 3D morphological closing of the occupied mask. Newly closed voxels that were previously free/ignore are filled with the modal class when modal support is strong (at least 4 agreeing neighbors). To fill slightly larger semantic cavities, we use a stricter criterion and only fill free/ignore voxels when the neighborhood is dense ( $n_{\text{occ}}(v) \geq 10$ ) and the modal support is high (at least 5 votes).

**(2) Warmup ego completion.** When temporal evidence is limited in early causal frames, we optionally complete the near-ego blind region by filling unknown near-ground voxels as 'driveable surface'. We consider voxels within radius  $r_{\text{ego}}$  around the ego

and fill them as driveable only if they are close to existing driveable evidence (via a small planar dilation) and not adjacent to object voxels (via a small 3D dilation), to avoid hallucinating structures near vehicles or pedestrians.

**(3) Conservative neighborhood coherence.** We perform a single coherence pass on occupied voxels. Voxels are *frozen* if they are reliable according to voxel evidence (e.g.,  $\text{conf}(v) \geq 0.75$  or  $p_{\text{occ}}(v) \geq 0.85$ ), and we also protect object and thin classes from being overwritten. For the remaining ambiguous occupied voxels, we update the label to the modal class only when neighborhood agreement is both strong and dominant (modal support  $\geq 5$  and modal votes form a clear majority, e.g.,  $\text{support}_{\text{mode}}(v) \geq 0.6 n_{\text{occ}}(v)$ ).

**(4) Background cleanup and instance dilation.** Finally, any residual ignore-labeled voxels are reassigned to the modal class when supported (at least 2 agreeing neighbors). To reduce small unlabeled gaps in thing instances, we apply a class-constrained instance dilation of radius  $\delta = 2$  voxels: within each thing semantic region, unassigned instance voxels inherit the nearest instance id (in 3D Euclidean distance) from nearby assigned voxels, improving instance completeness under occlusions and sparse sampling.

## 4 Experiments

We study FreeOcc under three complementary regimes. First, we evaluate the strict train-free setting, which is the main contribution of this work: no target-domain occupancy model is trained, and predictions are produced directly from foundation-model inference and geometric fusion. Second, for comparison with prior pseudo-label pipelines in the weakly supervised setting, we compare our train-free results, but also train downstream STCOcc models from generated pseudo-labels. Third, we report panoptic occupancy prediction performance, thus establishing baselines for train-free and weakly supervised panoptic occupancy prediction. Finally, we perform module-level ablations to analyze where the gains come from and which parts of the pipeline matter most.

We evaluate on Occ3D-nuScenes [13]. Regrettably, no official test set is available for this dataset. We follow the standard practice and report results on the 150 scene validation split. For panoptic occupancy, we follow the SparseOcc protocol [11] to generate instance voxel labels from nuScenes [3]. For semantic occupancy, we report mIoU, IoU<sub>occ</sub>, and RayIoU (including RayIoU<sub>1m</sub>, RayIoU<sub>2m</sub>, and RayIoU<sub>4m</sub>): mIoU captures voxel-level semantic overlap, IoU<sub>occ</sub> captures binary occupancy, and RayIoU more robustly evaluates semantic performance. For panoptic occupancy, we report RayPQ and its range-specific variants as defined in [11], which jointly penalize semantic, instance, and geometric errors. To guarantee reproducibility, we directly use the official evaluation code from SparseOcc [11] for all metrics.

### 4.1 Implementation Details

Unless stated otherwise, all reported train-free results are causal, i.e. only past and current frames are used for each timestamp. All hyperparameters are fixed and reused across runs after tuning on a set of 30 training scenes:  $\tau_C = 1e-5$ ,

$d_{\min} = 1$ ,  $d_{\max} = 50$ , merging threshold  $\tau_{ov} = 0.45$  (Intersection-over-Smaller-Volume), grid bounds  $(X, Y, Z) = (-40, 40) \times (-40, 40) \times (-10, 10)$ , voxel size  $s_v = 0.4\text{m}$ , vertical offset  $z_0 = -1\text{m}$ , and dilation radius  $\delta = 2$ . We do not retune parameters per comparison method or per metric. Full implementation details will be made publicly available.

For weakly supervised comparison, we additionally train downstream STCOcc models [10] from pseudo-labels generated by our pipeline in non-causal mode (future frames contributing to current prediction). We keep the official STCOcc training protocol (2 GPUs, batch size 8, 12 epochs) for the weakly supervised experiment.

For the panoptic occupancy prediction experiment, we extend STCOcc to jointly predict voxel semantics and instance IDs. The resulting model denoted STCOcc\_pano, inspired by SparseOcc’s instance prediction, reuses STCOcc’s sparse 3D BEV/voxel backbone and adds an instance-aware voxel head, panoptic label loading, and instance supervision (center focal-BCE + offset L1).

## 4.2 Main Results

**Table 1:** Training-free semantic occupancy prediction performance on Occ3D-nuScenes validation set. IoU per class and mIoU are reported. ‘others’ and ‘other\_flat’ classes are not included in the mIoU calculation. \* means that the method is from a preprint.

Method	mIoU	occupied	barrier	bicycle	bus	car	cons. veh.	motorcycle	pedestrian	traffic cone	trailer	truck	driv. surf.	sidewalk	terrain	manmade	vegetation
ShelfOcc* [2]	9.6	26.0	6.6	3.3	7.0	8.8	2.6	4.7	5.0	<b>8.1</b>	0.1	5.4	34.6	14.6	18.2	10.9	14.5
FreeOcc (Ours)	<b>16.9</b>	<b>37.2</b>	<b>16.1</b>	<b>7.0</b>	<b>12.2</b>	<b>17.6</b>	<b>13.0</b>	<b>8.4</b>	<b>9.7</b>	4.6	<b>2.1</b>	<b>14.0</b>	<b>51.3</b>	<b>31.1</b>	<b>29.0</b>	<b>17.7</b>	<b>19.4</b>

Table 1 compares IoU results in the train-free setting. The only comparable baseline is ShelfOcc without downstream training [2]. FreeOcc improves mIoU from 9.6 to 16.9 (+7.3 points), while also improving occupancy IoU (26.0 to 37.2). The gain is broad across most classes. Large improvements are observed on both object and structure categories, e.g. car (+8.8), truck (+8.6), construction vehicle (+10.4), driveable surface (+16.7), sidewalk (+16.5), terrain (+10.8), and manmade (+6.8). The only class where our score is lower is traffic cone, which remains a difficult small-object class in coarse voxel grids. Overall, this indicates that the training-free pipeline provides strong and well-calibrated semantic occupancy priors even without any downstream training and no access to target domain images.

The weakly supervised comparison table 2 extends the analysis beyond the strict train-free setting. In train-free mode, FreeOcc reaches 16.9 mIoU and 16.5 RayIoU, which is very close to GaussianFlowOcc [1] in mIoU (17.1), on par in

**Table 2:** Weakly-supervised semantic occupancy prediction performance on Occ3D-nuScenes validation set. IoU per class and mIoU are reported. ‘others’ and ‘other\_flat’ classes are not included in the mIoU calculation. \* means that the method is from a preprint.

Method	Train		mIoU	IoU <sub>occ</sub>	RayIoU	1m	2m	4m
	Free	Cam. Masks						
EasyOcc* [5]	×	✓	16.0	38.9	-	-	-	-
GaussianFlowOcc [1]	×	✓	17.1	13.9	16.5	11.8	16.6	21.0
ShelfOcc* [2]	×	×	9.6	26.0	-	-	-	-
ShelfOcc* [2] (+STCOcc [10])	×	✓	22.9	56.1	20.0	14.4	20.1	25.5
FreeOcc (Ours)	✓	×	16.9	37.2	16.5	11.7	16.7	21.6
FreeOcc (+STCOcc [10])	×	×	22.8	43.8	21.1	13.6	21.3	28.5

overall RayIoU (16.5 vs. 16.5), and slightly better at longer ranges (RayIoU<sub>2m</sub>: 16.7 vs. 16.6, RayIoU<sub>4m</sub>: 21.6 vs. 21.0).

When we use our labels for downstream training, FreeOcc+STCOcc reaches 22.8 mIoU, close to ShelfOcc+STCOcc (22.9), and improves RayIoU from 20.0 to 21.1. We note that longer range RayIoU metrics are significantly improved (RayIoU<sub>2m</sub>: 21.3 vs. 20.1, RayIoU<sub>4m</sub>: 28.5 vs. 25.5), while the near-range RayIoU<sub>1m</sub> remains slightly lower (13.6 vs. 14.4).

A key setup difference is that our transfer results do not use camera-visibility masks during downstream training. ShelfOcc generates visibility masks for pseudo-labels, which help to focus the training on visible parts. The authors report a large performance drop without these masks (13.4 mIoU vs. 22.9 mIoU with masks). This may explain ShelfOcc’s advantage in voxel mIoU, while FreeOcc dominates RayIoU, especially for long ranges where there may be more hidden parts. We claim that training without them may also lead to more reliable results beyond the benchmark metrics, since masking non-visible parts removes all incentives for the model to make correct predictions for those parts as well.

**Table 3:** Panoptic occupancy prediction on Occ3D-nuScenes’ validation set. Measured with RayPQ from [11].

Method	Sup.	RayPQ	RayPQ <sub>1m</sub>	RayPQ <sub>2m</sub>	RayPQ <sub>4m</sub>
SparseOcc [11]	Full	14.1	10.2	14.5	17.6
Panoptic-FlashOcc [16]	Full	16.0	11.9	16.3	19.7
FreeOcc (Ours)	Train-free	3.1	0.8	2.6	5.8
FreeOcc (+STCOcc [10])	Weak	3.9	1.0	3.0	7.6

The panoptic results table 3 reports panoptic occupancy performance. In train-free mode, FreeOcc reaches 3.1 RayPQ; with weak supervision through STCOcc\_pano, performance increases to 3.9 RayPQ.

Absolute RayPQ remains lower than fully supervised methods, but the range-wise behavior is informative: RayPQ<sub>4m</sub> is 103% higher than global RayPQ, while the same comparison is 23% for Panoptic-FlashOcc, indicating that geometric alignment quality is a dominant factor in FreeOcc’s performance. This is consistent with the strict RayPQ matching criterion, where correct panoptic assignment requires both semantic consistency and sufficient occupancy overlap. True Positives are accounted only if the IoU between the predicted segment and the ground truth segment is above a threshold of 50%, which is a hard target for weakly supervised methods even if instances are well detected and separated. We therefore position these numbers as a first training-free/weakly supervised panoptic baseline and a concrete starting point for future refinements.

**Table 4: Ablation study.** Five stages of ablation are presented where features are added incrementally. (I) only includes the Semantic and Geometric branches. (V) is the final FreeOcc method. All values are computed on the Occ3D-nuScenes validation set.

Stage	Prompts & Rules	Conf. Filter	Occ Refine	Inst. Ident.	mIoU	RayIoU	RayPQ
(I)					10.9	11.2	1.1
(II)	✓				13.6	14.2	1.4
(III)	✓	✓			13.7	14.2	1.4
(IV)	✓	✓	✓		15.8	14.6	1.5
(V)	✓	✓	✓	✓	16.9	16.5	2.5

Table 4 confirms the contribution of each module. Starting from the semantic+geometric branches (Stage I), prompt/rule semantics already provide a large gain (Stage II), and occupancy refinement further improves semantic quality (Stage IV). Numerically, Stage I  $\rightarrow$  II brings +2.7 mIoU, +2.9 RayIoU, and +0.3 RayPQ, showing that semantic prompt design is a primary driver, and changes as simple as synonyms may significantly impact performance. Stage II  $\rightarrow$  III is nearly unchanged, indicating that confidence filtering mostly stabilizes outputs rather than shifting aggregate metrics. Stage III  $\rightarrow$  IV contributes +2.1 mIoU and +0.5 RayIoU through voxel refinement. The full model (Stage V) performs best on all reported metrics, and the instance-identification stage provides the largest panoptic jump (RayPQ 1.5  $\rightarrow$  2.5), while also improving RayIoU (14.6  $\rightarrow$  16.5). Overall, Stage I  $\rightarrow$  V yields +6.0 mIoU, +5.3 RayIoU, and +1.4 RayPQ.

Table 5 provides insights about two other factors: camera-pose priors and causality constraints. Removing extrinsics (no camera poses to MapAnything) significantly degrades performance: mIoU drops by 53%, RayIoU by 44%, and RayPQ by 56%. This highlights that while the method is training-free and open-vocabulary, accurate poses are still important for reliable 3D fusion, and closing this gap is an interesting direction for future work. Using future frames (non-causal) improves voxel mIoU by 21% but increases RayIoU by only 1.8%. This suggests that denser temporal accumulation adds volumetric coverage but does

**Table 5:** Impact of ablating prior extrinsics (no camera poses given to MapAnything as input) and causality (using future frames for current prediction) on panoptic occupancy prediction. Values are reported for Occ3D-nuScenes’ validation set.

Extrinsics	Causal	mIoU	RayIoU	RayPQ
✓	✓	16.9	16.5	2.5
×	✓	7.9	9.2	1.1
✓	×	20.4	16.8	3.5

not necessarily improve geometric and semantic accuracy beyond a certain point, given that RayIoU is specifically designed to be robust to geometric cheating with thick surfaces.

## 5 Conclusion

We presented FreeOcc, a training-free pipeline for camera-only semantic and panoptic occupancy prediction that combines promptable 2D priors with foundation-model 3D reconstruction. The method can operate without any downstream training, requires no target data, and preserves the prompt-driven flexibility of the open-vocabulary foundation models. In this setting, FreeOcc matches the performance of trained pipelines on Occ3D-nuScenes, and when used as a pseudo-label generator with minimal adaptations, surpasses state-of-the-art methods in RayIoU. FreeOcc also sets the first training-free and weakly supervised panoptic occupancy prediction baselines.

Overall, the experiments support three points:

1. Train-free occupancy prediction is made possible, with FreeOcc’s performance being competitive with trained weakly supervised pipelines.
2. Panoptic occupancy is feasible without dense 3D supervision.
3. At the same time, the remaining panoptic gap to fully supervised methods highlights that geometry quality and precise volumetric alignment remain the main bottlenecks in this label-free regime.

We hope that future works will explore sensor extrinsics-free performance, which is currently significantly lower, in order to advance towards even more generalizable occupancy prediction methods, requiring only camera input.

## References

1. Boeder, S., Gigengack, F., Risse, B.: GaussianFlowOcc: Sparse and Weakly Supervised Occupancy Estimation using Gaussian Splatting and Temporal Flow (Aug 2025). <https://doi.org/10.48550/arXiv.2502.17288>, <http://arxiv.org/abs/2502.17288>, arXiv:2502.17288 [cs]

2. Boeder, S., Gigengack, F., Roesler, S., Caesar, H., Risse, B.: ShelfOcc: Native 3D Supervision beyond LiDAR for Vision-Based Occupancy Estimation (Nov 2025). <https://doi.org/10.48550/arXiv.2511.15396>, <http://arxiv.org/abs/2511.15396>, arXiv:2511.15396 [cs]
3. Caesar, H., Bankiti, V., Lang, A.H., Vora, S., Liong, V.E., Xu, Q., Krishnan, A., Pan, Y., Baldan, G., Beijbom, O.: nuScenes: A multimodal dataset for autonomous driving (May 2020). <https://doi.org/10.48550/arXiv.1903.11027>, <http://arxiv.org/abs/1903.11027>, arXiv:1903.11027 [cs, stat]
4. Gan, W., Liu, F., Xu, H., Mo, N., Yokoya, N.: GaussianOcc: Fully Self-supervised and Efficient 3D Occupancy Estimation with Gaussian Splatting (Jul 2025). <https://doi.org/10.48550/arXiv.2408.11447>, <http://arxiv.org/abs/2408.11447>, arXiv:2408.11447 [cs]
5. Hayes, S., Sistu, G., Eising, C.: EasyOcc: 3D Pseudo-Label Supervision for Fully Self-Supervised Semantic Occupancy Prediction Models (Nov 2025). <https://doi.org/10.48550/arXiv.2509.26087>, <http://arxiv.org/abs/2509.26087>, arXiv:2509.26087 [cs]
6. Huang, Y., Zheng, W., Zhang, Y., Zhou, J., Lu, J.: Tri-Perspective View for Vision-Based 3D Semantic Occupancy Prediction. 2023 IEEE/CVF Conference on Computer Vision and Pattern Recognition (CVPR) pp. 9223–9232 (Jun 2023). <https://doi.org/10.1109/CVPR52729.2023.00890>, <https://ieeexplore.ieee.org/document/10203437/>, conference Name: 2023 IEEE/CVF Conference on Computer Vision and Pattern Recognition (CVPR) ISBN: 9798350301298 Place: Vancouver, BC, Canada
7. Jiang, H., Liu, L., Cheng, T., Wang, X., Lin, T., Su, Z., Liu, W., Wang, X.: GaussTR: Foundation Model-Aligned Gaussian Transformer for Self-Supervised 3D Spatial Understanding (Mar 2025). <https://doi.org/10.48550/arXiv.2412.13193>, <http://arxiv.org/abs/2412.13193>, arXiv:2412.13193 [cs]
8. Keetha, N., Müller, N., Schönberger, J., Porzi, L., Zhang, Y., Fischer, T., Knapitsch, A., Zauss, D., Weber, E., Antunes, N., Luiten, J., Lopez-Antequera, M., Bulò, S.R., Richardt, C., Ramanan, D., Scherer, S., Kotschieder, P.: MapAnything: Universal Feed-Forward Metric 3D Reconstruction [mapanything.github.io](https://github.com/mapanything)
9. Kirillov, A., Mintun, E., Ravi, N., Mao, H., Rolland, C., Gustafson, L., Xiao, T., Whitehead, S., Berg, A.C., Lo, W.Y., Dollár, P., Girshick, R.: Segment Anything (Apr 2023). <https://doi.org/10.48550/arXiv.2304.02643>, <http://arxiv.org/abs/2304.02643>, arXiv:2304.02643 [cs]
10. Liao, Z., Wei, P., Chen, S., Wang, H., Ren, Z.: STCOcc: Sparse Spatial-Temporal Cascade Renovation for 3D Occupancy and Scene Flow Prediction (Apr 2025). <https://doi.org/10.48550/arXiv.2504.19749>, <http://arxiv.org/abs/2504.19749>, arXiv:2504.19749 [cs]
11. Liu, H., Chen, Y., Wang, H., Yang, Z., Li, T., Zeng, J., Chen, L., Li, H., Wang, L.: Fully Sparse 3D Occupancy Prediction (Jul 2024). <https://doi.org/10.48550/arXiv.2312.17118>, <http://arxiv.org/abs/2312.17118>, arXiv:2312.17118 [cs]
12. Pan, M., Liu, J., Zhang, R., Huang, P., Li, X., Wang, B., Xie, H., Liu, L., Zhang, S.: RenderOcc: Vision-Centric 3D Occupancy Prediction with 2D Rendering Supervision (Mar 2024). <https://doi.org/10.48550/arXiv.2309.09502>, <http://arxiv.org/abs/2309.09502>, arXiv:2309.09502 [cs]
13. Tian, X., Jiang, T., Yun, L., Mao, Y., Yang, H., Wang, Y., Wang, Y., Zhao, H.: Occ3D: A Large-Scale 3D Occupancy Prediction Benchmark for Autonomous Driving (Dec 2023). <https://doi.org/10.48550/arXiv.2304.14365>, <http://arxiv.org/abs/2304.14365>, arXiv:2304.14365 [cs]

14. Wang, J., Liu, Z., Meng, Q., Yan, L., Wang, K., Yang, J., Liu, W., Hou, Q., Cheng, M.M.: OPUS: Occupancy Prediction Using a Sparse Set
15. Wei, Y., Zhao, L., Zheng, W., Zhu, Z., Zhou, J., Lu, J.: SurroundOcc: Multi-Camera 3D Occupancy Prediction for Autonomous Driving (Aug 2023). <https://doi.org/10.48550/arXiv.2303.09551>, <http://arxiv.org/abs/2303.09551>, arXiv:2303.09551 [cs]
16. Yu, Z., Shu, C., Sun, Q., Bian, Y., Wei, X., Yu, J., Liu, Z., Yang, D., Li, H., Chen, Y.: Panoptic-FlashOcc: An Efficient Baseline to Marry Semantic Occupancy with Panoptic via Instance Center (Oct 2024). <https://doi.org/10.48550/arXiv.2406.10527>, <http://arxiv.org/abs/2406.10527>, arXiv:2406.10527 [cs]
17. Zhang, C., Yan, J., Wei, Y., Li, J., Liu, L., Tang, Y., Duan, Y., Lu, J.: OccNeRF: Advancing 3D Occupancy Prediction in LiDAR-Free Environments (Aug 2024). <https://doi.org/10.48550/arXiv.2312.09243>, <http://arxiv.org/abs/2312.09243>, arXiv:2312.09243 [cs]